Analytical and Bioanalytical Chemistry (2019) 411:4729–4737
https://doi.org/10.1007/s00216-018-1447-2

RESEARCH PAPER

Corona discharge electrospray ionization of formate-containing solutions enables in-source reduction of disulfide bonds

Bradley B. Stocks[1] · Jeremy E. Melanson[1]

Received: 6 September 2018 / Revised: 12 October 2018 / Accepted: 22 October 2018 / Published online: 6 November 2018

Abstract

Disulfide bonds are critical linkages for maintaining protein structure and enzyme activity. These linkages, however, can limit peptide sequencing efforts by mass spectrometry (MS) and often require chemical reduction and alkylation. Under such conditions, information regarding cysteine connectivity is lost. Online partial disulfide reduction within the electrospray (ESI) source has recently been established as a means to identify complex cysteine linkage patterns in a liquid chromatography-MS experiment without the need for sample pre-treatment. Corona discharge (CD) is invoked as the causative factor of this in-source reduction (ISR); however, evidence remains largely circumstantial. In this study, we demonstrate that instrumental factors—nebulizing gas, ESI capillary material, organic solvent content, ESI spray needle-to-MS distance—all modulate the degree of reduction observed for the single disulfide in oxytocin, further implicating CD in ISR. Rigorous analysis of solution conditions, however, reveals that corona discharge alone can induce only minor disulfide reduction. We establish that CD-ESI of peptide solutions containing formic acid or its conjugate base results in a dramatic increase in disulfide reduction. It is also determined that ISR is exacerbated at low pH for complex peptides containing multiple disulfide bonds and possessing higher-order structure, as well as for a small protein. Overall, our results demonstrate that ESI of formate/formic acid–containing solutions under corona discharge conditions facilitates disulfide ISR, likely by a similar reduction pathway measured in γ-radiolysis studies nearly three decades ago.

Keywords Disulfide bond · In-source reduction · Formate · Corona discharge · Electrospray ionization

Introduction

Electrospray ionization mass spectrometry (ESI-MS) is widely applicable to biomolecule analysis [1], and under controlled conditions allows detection of native proteins and intact protein complexes [2, 3]. Multiple instrument voltage and temperature settings can, however, alter protein conformation [4], induce amino acid modifications [5, 6], and cause analyte fragmentation [7]. One parameter that attracts much attention is the voltage applied to the ESI capillary, due to the potential for electric discharge. Corona discharge (CD) results from breakdown of the nebulizer gas used to enhance solvent evaporation during electrospray. Under extreme conditions, CD can be visually detected [8]; however, such regimes are often avoided due to the degradation of analyte signal [9]. Corona discharge leads to the production of reactive species, such as hydroxyl radical (•OH), within the ion source [10]. Hydroxyl radical oxidizes amino acid side chains during CD-ESI [5, 11] and readily reacts with a myriad of other organic molecules [12].

Disulfide bonds are crucial protein post-translational modifications [13]; however, they hinder facile peptide sequencing efforts. Typical protein characterization by liquid chromatography (LC)-MS therefore generally includes time-consuming chemical reduction and alkylation steps, abolishing cysteine connectivity information in the process [14]. Oxidative disulfide cleavage during ESI can be facilitated through interaction with a helium plasma [15] or by UV irradiation [16], thus eliminating the need for sample pre-treatment. Disulfide reduction represents another option, and reduction can be performed online with the use of an electrochemical cell [17], or

Published in the topical collection *Young Investigators in (Bio-)Analytical Chemistry* with guest editors Erin Baker, Kerstin Leopold, Francesco Ricci, and Wei Wang.

Electronic supplementary material The online version of this article (https://doi.org/10.1007/s00216-018-1447-2) contains supplementary material, which is available to authorized users.

✉ Bradley B. Stocks
bradley.stocks@nrc-cnrc.gc.ca

[1] National Research Council Canada, Metrology, 1200 Montreal Road, Ottawa, ON K1A 0R6, Canada

within the ESI plume itself [18]. This in-source reduction (ISR) approach has demonstrated utility in the elucidation of complex cysteine linkage patterns in an LC-MS workflow [19, 20]. Each disulfide reduction increases the analyte mass by 2 Da; therefore, ISR of a simple peptide is readily observed in the mass spectrum by monitoring distortions to the isotopic envelope. The addition of ion mobility can facilitate detection for more complex sequences [21]. The potential value of ISR is evident, but details regarding the mechanism by which it proceeds are scarce. All accounts to date [18–21] suggest that CD within the ESI source is a contributing factor to the reduction, consistent with a recent report of corona-induced reduction of quinone derivatives in positive-mode ESI [22]; however, little direct evidence has been presented.

This work investigates various ESI-MS parameters known to modulate corona discharge, as well as multiple solution conditions, to further understand the mechanism of disulfide ISR. Using parameters under which we have previously observed ISR [21], disulfide reduction is abolished when the nebulizing gas is changed from N_2 to SF_6, a demonstrated suppressant of corona discharge at moderate ESI voltages [5, 9, 22]. In agreement with earlier reports [18, 19], we observe a protective effect with increasing acetonitrile percentage in the spray solvent. However, when trifluoroacetic acid is substituted for formic acid in LC solvents, no ISR is detected, even in the absence of organic modifier. This observation spurred a rigorous examination of solution conditions, altering the electrolyte identity and concentration, as well as the acid used for titration. Reduction of the single disulfide in oxytocin is observed predominantly in solutions containing formic acid or its conjugate base and is largely independent of pH. Acidic pH, however, does facilitate increased ISR of complex polypeptides insulin and hepcidin, as well as lysozyme, likely due to increased disulfide solvent accessibility resulting from higher-order structure disruption. Key experiments repeated on a second MS system demonstrate a reasonable degree of instrument independence. Overall, our results are reminiscent of disulfide reduction observed during γ-radiolysis of formate-containing solutions [23–26]. These reports invoke a reduction mechanism mediated by carboxyl radical anion, formed upon H abstraction from formate/formic acid by hydroxyl radical. We thus propose that a similar mechanism is extant during CD-ESI of formate-containing solutions and is responsible for disulfide ISR.

Experimental

Chemicals and reagents

Ammonium acetate, ammonium formate, HCl, trifluoroacetic acid, and LC-MS grade formic acid were obtained from Fisher Scientific (Nepean, ON). Hen egg white lysozyme, ammonium bicarbonate, dithiothreitol, and bovine insulin were purchased from Sigma (St. Louis, MO). Glacial acetic acid was obtained from ACP Chemicals (Montreal, QC). Human hepcidin was from AnaSpec (Fremont, CA) and oxytocin was from the U.S. Pharmacopeia (Rockville, MD). Eighteen MΩ deionized water was produced in-house with a Milli-Q system.

Mass spectrometry

Peptides were dissolved to 2 μM in 10 mM ammonium buffer, where the counter ion was either acetate (pH 6.7), formate (pH 6.7), or bicarbonate (pH 7.9). For acidic solutions, buffers were titrated to pH 2.7 with formic acid, HCl, or trifluoroacetic acid (TFA). Ten μM lysozyme was prepared in acetate and formate buffers, and titration was done with formic acid. Key solutions referenced throughout this report were prepared as follows: solution **1**—10 mM ammonium acetate, pH 6.7; solution **2**—10 mM ammonium acetate + 80 mM formic acid, pH 2.7; solution **3**—10 mM ammonium formate, pH 6.7; solution **4**—100 mM ammonium formate, pH 6.7; solution **5**—10 mM ammonium formate + 90 mM formic acid, pH 2.7. Chemically reduced, positive control lysozyme samples were prepared by incubation with 25 mM DTT at 70 °C for 5 or 30 min. For conventional ESI experiments, solutions were infused at 1–50 μL min^{-1} using a syringe pump (Harvard Apparatus, South Natick, MA) into a Waters (Milford, MA) Synapt G2 Q-TOF mass spectrometer operating in positive ionization mode. Source and IMS parameters were used as described previously [21]. Briefly, the capillary voltage was operated between 2 and 4 kV while the cone and extraction cone voltages were kept at 20 and 2 V, respectively. The IMS cell was pressurized with ~ 3 mbar N_2, and the IMS traveling-wave ion guide was operated at 800 m s^{-1} with a wave height of 40 V; protein experiments were carried out at 600 m s^{-1} and 30 V. Nebulizer gas experiments used either N_2 (MEGS, Nepean, ON) or SF_6 (Praxair, Mississauga, ON). Arrival time distributions and mass spectra were extracted using MassLynx 4.1 software and lysozyme collision cross sections (CCS) were determined using previously described calibration procedures [27]. Theoretical peptide isotopologue *m/z* values and relative abundances for native oxytocin ($C_{43}H_{66}N_{12}O_{12}S_2$) were determined using the online IUPAC Molecular Weight Calculator (http://www.ciaaw.org/calculators). One thousand Monte Carlo iterations resulted in a native oxytocin M+2 isotopologue theoretical abundance of 0.2575 ± 0.015, consistent with that determined using the ProteinProspector web tool [28]. The predominant outcome of peptide ISR is protonated cysteines [19]; thus, each disulfide reduction increased by two the number of hydrogens in the peptide molecular formula for isotopic envelope fitting, performed as described previously [21].

Nano-electrospray experiments were conducted using the Synapt NanoLockspray source. Applied N_2 backing pressure of 0.3 bar enabled peptide solutions to be sprayed from gold-coated borosilicate capillaries (Waters) at a flow rate of ~30 nL min^{-1}, as determined gravimetrically. Stable spray conditions were maintained while the capillary voltage was controlled between 1.2 and 2.5 kV. Images in Fig. S2 (see Electronic Supplementary Material (ESM)) were taken with the embedded camera in the NanoLockspray source.

The effects of organic solvents on ISR were investigated by liquid chromatography (LC) using a Waters Acquity UPLC. Solvents were water/acetonitrile with 0.1% of either formic or trifluoroacetic acid. Peptide samples were prepared at 40 μM in water. LC solvent (95 μL min^{-1}) was combined with peptide sample (5 μL min^{-1}, syringe pump) in a mixing tee, and the resulting solution was directed into the ESI source of the mass spectrometer with the capillary voltage held at 4 kV. Acetonitrile percentages depicted in Fig. 2 refer to post-mixing values.

Oxytocin and insulin experiments using selected solution conditions were also conducted on an Orbitrap Fusion Lumos (Thermo Scientific, San Jose, CA), with the heated-ESI source operating in positive mode. For infusion experiments, the ESI capillary was controlled between 2 and 4 kV, with the sheath, auxiliary, and sweep gases held at 175, 385, and 80 L h^{-1}, respectively. The ion transfer tube and vaporizer temperatures were set to 300 and 40 °C, respectively. The Orbitrap was operated at a mass resolution of 30,000, with an RF of 40%, an AGC target of 4.0×10^5, and a maximum injection time of 100 ms. LC experiments were carried out as described above, albeit with the use of a Thermo Vanquish UHPLC. All MS parameters were identical to those used for infusion, except for the sheath and sweep gas flows (105 and 0 L h^{-1}, respectively), and the vaporizer temperature (135 °C) [20].

Results and discussion

Corona discharge required for in-source reduction

Corona discharge has been reported as a significant contributor to disulfide reduction within the electrospray source. Many experimental variables are known to affect the onset of CD, and in the following paragraphs, we investigate a number of them—nebulizer gas, spray needle material, organic solvent content—to determine their effects on oxytocin (OT) reduction. In previous work [21], we monitored OT reduction by the increase in the M+2 isotopologue abundance due to the addition of two hydrogens. In the ensuing sections, we refer to the abundance of the OT M+2 peak relative to the monoisotopic peak, OT_{M+2}, as a measure of disulfide reduction.

We previously demonstrated peptide ISR on a Q-TOF instrument [21], although other studies have used Orbitrap [19, 20] and FT-ICR [18] mass spectrometers. Results reported below were predominantly acquired using the Synapt G2; however, key experiments were repeated on the Orbitrap Fusion Lumos. Corona discharge during ESI is often visually detected by its characteristic blue emission [8, 29] and was clearly visible within the ESI source on the Synapt at 4 kV; however, visual detection on the Lumos required increasing the capillary voltage to 6 kV. Differences in source geometries likely contribute to such inter-platform discrepancies and account, at least in part, for the variance in ISR magnitude measured between the two MS systems.

Effect of nebulizer gas Earlier MS studies of disulfide ISR have postulated that CD is a causative factor, while utilizing N_2 as a nebulizing gas [19–21]. Employing SF_6 in place of N_2 can suppress electric discharge [9] and has been shown to reduce corona-induced protein oxidation [5] and quinone reduction [22]. As we have previously demonstrated [21], OT dissolved in 10 mM ammonium acetate, pH 6.7 (solution **1**) and electrosprayed at 4 kV resulted in no ISR; however, when titrated to pH 2.7 (solution **2**), a dramatic increase in reduction became apparent (Fig. 1a). These experiments were performed using N_2 as the ESI nebulizing gas, which has been demonstrated to undergo dielectric breakdown above 3 kV [5]. However, exchanging the nebulizer gas for SF_6 resulted in no discernable OT reduction at 4 kV, regardless of solution conditions (Fig. 1b). Further, CD can be modulated by the distance between the ESI capillary and the MS [22], and Fig. S1 (see ESM) shows that decreasing the capillary-to-MS distance resulted in an increase in the detected OT reduction. The results of Fig. 1 and ESM Fig. S1 implicate corona discharge as a causative factor in disulfide ISR, although do not discount contributions from additional sources.

Effect of capillary material To investigate additional elements potentially responsible for disulfide ISR [19, 20], we infused OT solutions from borosilicate glass nano-ESI capillaries. This alleviates concerns of electrochemical reactions occurring at the surface of the stainless steel spray needle in the standard ESI source [30, 31]. Figure S2 (see ESM) shows images of the nanospray capillary taken under darkness with increasing applied voltage. Corona discharge was not visually detected at 1.2 kV, became observable at 2.5 kV, and was readily apparent at 4 kV. Unfortunately, spray instability at 4 kV precluded OT data acquisition. The open architecture of the nanospray source and the lack of a nebulizing gas flow result in an ambient air environment surrounding the spray capillary. It should be noted that corona discharge in air requires higher voltage than in nitrogen [32], likely due to electron scavenging properties of oxygen [5, 33]. When OT was sprayed from solution **2** at 1.2 kV, the OT_{M+2} ratio was 0.26, indistinguishable from the theoretical value (Fig. S3). A slight increase to 0.32 was observed at 2.5 kV, coupled with an

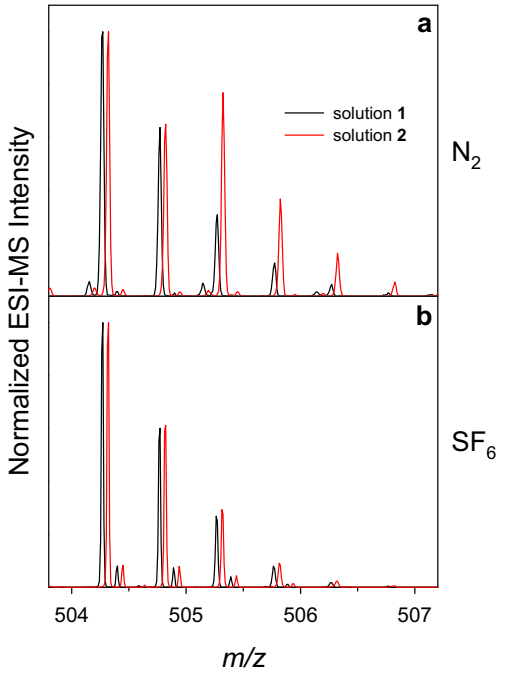

Fig. 1 Effect of nebulizing gas on oxytocin ISR. OT in solution **1** (10 mM ammonium acetate, pH 6.7, black line) or solution **2** (10 mM ammonium acetate + 80 mM formic acid, pH 2.7, red line, offset by 0.05 Da for clarity) sprayed with N_2 (a) or SF_6 (b). Solutions were infused at 5 μL min^{-1} and the ESI capillary voltage was 4 kV

increase in the OT_{M+1} ratio—a phenomenon not observed with the standard ESI source (Fig. 1a). Oxidative disulfide cleavage during ESI results in formation of thiol (–SH) and sulfinyl radical (–SO•) [15, 16]. Low abundance radical products (–S• HS–) have been reported in ISR as well [19], perhaps accounting for the increased OT_{M+1} shown in Fig. S3 (see ESM). The conventional ESI source employs a stainless steel capillary, enabling electrochemical reactions at the metal-solution interface [34], while such reactions are largely absent in the glass spray needle used in the nanospray source. The continued observation of disulfide ISR further asserts CD as a causative factor.

Effect of organic solvent Light emission from CD has been found to be significantly diminished with increasing percentage of organic modifier when compared to pure water [29]. Previous accounts of disulfide ISR have noted decreased reduction efficiency in the presence of organic solvent, i.e., acetonitrile in an LC gradient [18, 19], perhaps due to a suppression of CD. We infused OT into a stepped LC gradient, with solvent B being 0.1% formic acid in acetonitrile. In 100% solvent A (0.1% formic acid in water), the OT_{M+2} ratio was 0.7, nearly 3-fold higher than the theoretical value (Fig. 2). With increasing solvent B percentage, a steady decrease in ISR was measured, approaching the theoretical OT_{M+2} ratio at 50% ACN. We observed a similar trend in LC-Orbitrap experiments (ESM Fig. S4), and these results are in agreement with those of previous ISR studies [18, 19]. TFA can also be used in LC solvents for peptide and protein experiments [35, 36]; however, it remains less prevalent than formic acid due to potential ESI signal suppression [37]. When the OT experiments described above were repeated with 0.1% TFA in the LC solvents, no disulfide ISR was observed, even in the absence of organic solvent (Fig. 2). Corona discharge did not seem to be greatly affected however, as visual inspection of the ESI source under darkness revealed similar blue light emission regardless of which acid was used.

As a whole, investigation of parameters linked to corona discharge—capillary voltage, nebulizer gas, inter-electrode distance, organic solvent content—strongly suggests that it is required for disulfide ISR; however, the results of Fig. 2 intimate that an additional factor is also involved. We previously showed that solution pH can have a dramatic effect on the amount of peptide ISR [21], and in the ensuing section, we rigorously investigate solution parameters amenable to disulfide reduction.

Disulfide ISR: a formate-mediated process

Corona discharge occurs readily when aqueous solutions are exposed to elevated ESI voltages [10], and this is supported by the results of Fig. 3. While corona was visually detected when OT was sprayed from pure water, we measured minimal disulfide reduction except under the harshest conditions—low flow rate coupled with high ESI voltage (Fig. 3a). Pure water is not a common solvent for ESI; typically, a volatile electrolyte, such as ammonium acetate, is added in low-millimolar concentrations. Figure 3b shows that no significant increase in OT_{M+2} over the theoretical value occurs when the peptide is dissolved in solution **1** (10 mM ammonium acetate, pH 6.7), for any of the nine flow rate/voltage combinations tested. A

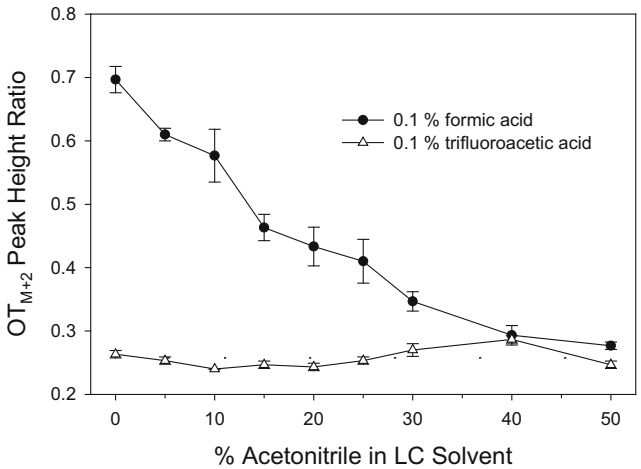

Fig. 2 Effect of organic modifier on disulfide ISR. Oxytocin M+2 isotopologue peak height as a function of acetonitrile percentage in LC solvent acidified with formic (filled circles) or trifluoroacetic (open triangles) acid. LC flow rate was 100 μL min^{-1} and ESI voltage was 4 kV. Dashed line indicates theoretical peak height. Error bars represent standard deviations of triplicate measurements

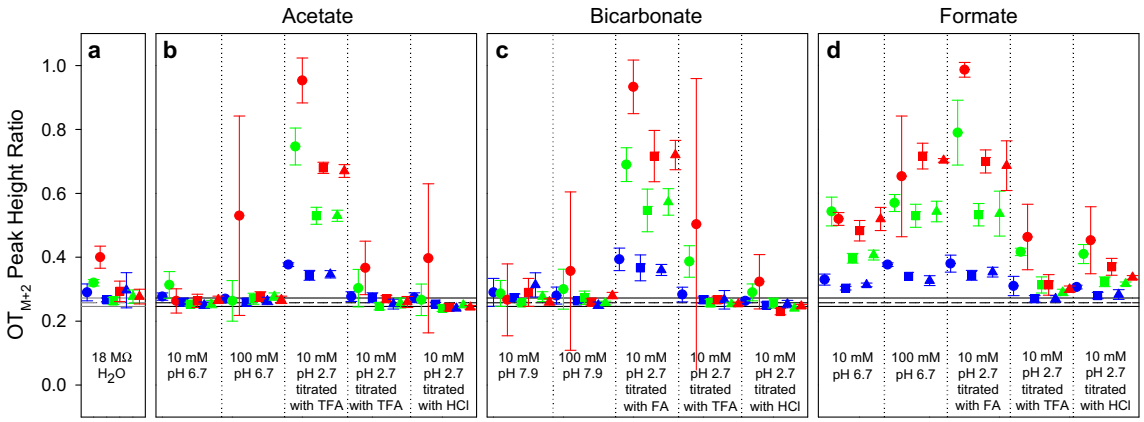

Fig. 3 Oxytocin M+2 isotopologue peak height relative to monoisotopic peak under various solution and ionization conditions. Panel (a) shows results for oxytocin dissolved in water. Remaining panels depict data for oxytocin in ammonium acetate (b), ammonium bicarbonate (c), or ammonium formate (d). Acidic solutions were titrated to pH 2.7 with either formic acid (FA), trifluoroacetic acid (TFA), or hydrochloric acid (HCl). Vertical dotted lines separate each different solution condition. Peptide solutions were infused at 1 μL min^{-1} (●), 10 μL min^{-1} (■), or 50 μL min^{-1} (▲). ESI capillary voltage was 2 kV (blue), 3 kV (green), or 4 kV (red). Horizontal black lines indicate the theoretical OT M+2 isotopologue peak height ± uncertainty, as determined in the "Experimental" section. Error bars represent standard deviations of triplicate measurements

positive correlation between electrolyte concentration and CD has been described [38]; however, we found negligible difference in OT reduction when sprayed from 10 or 100 mM ammonium acetate (Fig. 3b). The situation was markedly different when the ammonium acetate was titrated to pH 2.7 with formic acid (solution **2**), as we previously reported [21]. The OT$_{M+2}$ measured from solution **2** was 30–35% higher than that from solution **1** when sprayed at only 2 kV; more dramatic increases were seen at elevated voltages where visual detection of CD was possible. The highest amount of reduction was observed at 1 μL min^{-1}; however, spray instability at 4 kV likely contributed to the larger measurement error. Electrospray consistency and ISR levels appeared to stabilize upon increasing to 10 μL min^{-1} and above. We also observed an increase in OT$_{M+2}$ on the Fusion Lumos when comparing spectra obtained from solutions **1** and **2** at 4 kV (ESM Fig. S5). Remarkably, when alternative acids (TFA, HCl) were employed to titrate solution **1** to pH 2.7, the OT$_{M+2}$ profiles of Fig. 3b reverted back to that measured from solution **1** at neutral pH. Repetition with another volatile electrolyte, ammonium bicarbonate, yielded very similar results (Fig. 3c), albeit with slightly more variability. The fact that ISR was only observed when using formic acid prompted the experiments shown in Fig. 3d, using ammonium formate as the electrolyte. As disulfide reduction was measured for nearly all voltage/flow rate combinations, it became apparent that the formate/formic acid conjugate pair must play a role in ISR.

Radiolysis literature provides mechanistic link to ISR

Corona discharge during ESI of aqueous solutions produces hydroxyl radical (•OH) [39] which can readily oxidize biomolecules [5, 11], and we have observed minor amounts of oxytocin oxidation under CD conditions [21]. Hydroxyl radical is also formed upon water radiolysis and is a useful probe for protein structural analysis [40], however is efficiently scavenged by organic acids, such as formic and acetic acids, and their conjugate bases [12, 41]. Hydrogen abstraction from formate by •OH generates the carboxyl radical anion, $CO_2^{\bullet-}$, which has been shown to reduce proteins through selective electron donation to disulfides [42]. A number of studies have since described disulfide reduction resulting from γ-radiolysis of formate-containing solutions [23–26, 43], to which our ISR results elicit comparison.

To facilitate investigation into the analogous nature of the previous γ-radiolysis work with our ISR data, key data points from Fig. 3d were compiled. The most obvious trend in Fig. 4 shows that increasing ESI voltage when spraying formate-containing solutions resulted in elevated levels of disulfide reduction. More subtly, comparison of data from solutions **3** and **4** revealed that under CD conditions at high voltages, an increase in formate concentration resulted in a concomitant increase in ISR. Acetate also readily reacts with •OH [12] although carbon-centered radicals from non-formate salts do not react readily enough to reduce disulfides [44]. This is consistent with the fact that we observed no ISR when oxytocin was dissolved in only acetate/acetic acid (ESM Fig. S6). Additional scrutiny of the data acquired at 4 kV (Fig. 4) implied that at flow rates ≥ 10 μL min^{-1}, solution pH does not greatly affect the level of measured ISR. Under these conditions, the amounts of OT reduction observed from solution **4**, solution **5**, and LC were all in agreement. This appeared to contradict earlier ISR work [21]; however, the presence of acid imposed a large increase on disulfide reduction at the lowest flow rate tested. These findings are consistent with the radical chain reaction mechanism previously proposed

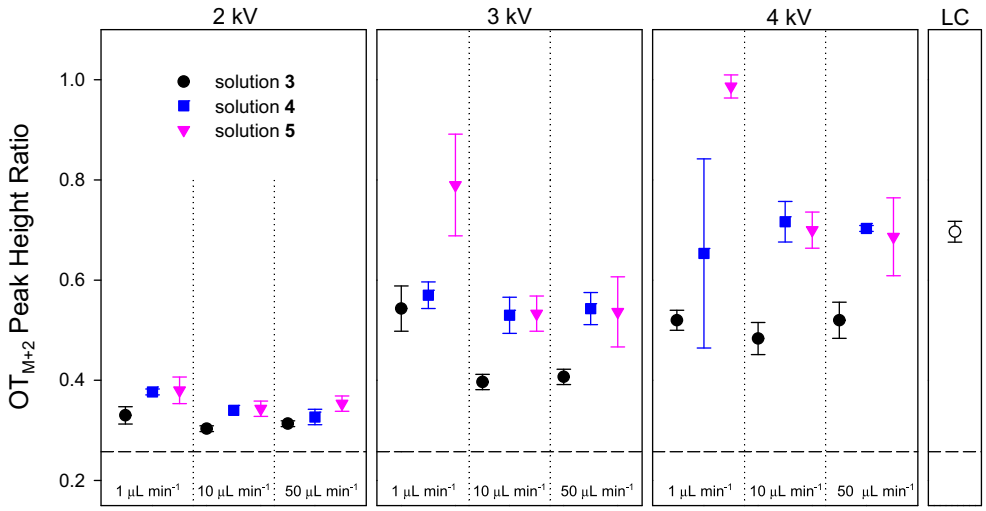

Fig. 4 Comparison of oxytocin ISR results from formate-containing solutions. 10 mM ammonium formate, pH 6.7 (solution **3**, black circles); 100 mM ammonium formate, pH 6.7 (solution **4**, blue squares); 10 mM ammonium formate titrated to pH 2.7 with formic acid (solution **5**, pink triangles) resulting in approximately 100 mM total formate concentration. Data points are segregated into panels by ESI capillary voltage (2, 3, 4 kV). Vertical dotted lines separate infusion flow rates of 1, 10, and 50 μL min^{-1}. Also shown is the LC value in 0% ACN at 4 kV from Fig. 1. LC flow rate was 100 μL min^{-1} and 0.1% formic acid in mobile phases corresponds to ~24 mM. Dashed line indicates the theoretical peak height ratio for the OT M+2 isotopologue. Error bars represent standard deviations of triplicate measurements

from radiolysis studies [25, 26], simplified in Scheme 1, whereby increasing formate concentration and decreasing pH both had positive effects on disulfide reduction. It is thus reasonable to propose that the disulfide ISR during ESI observed here and elsewhere [18–21] is mediated by $CO_2^{\bullet-}$, formed by proton abstraction from formate/formic acid by •OH produced via corona discharge.

Low pH enhances ISR of complex polypeptides

An interesting observation from previous radiolysis studies conveys the pH dependence of protein disulfide reduction, with the general trend towards increased reduction in acidic solutions [25, 26]. This is potentially due to the need for protonation of the disulfide radical anion (Scheme 1) and/or the acid-induced disruption of protein higher-order structure, allowing for increased solvent accessibility of disulfide bonds. As oxytocin is a relatively simple peptide (~1000 Da, 1 disulfide), we sought to test the pH effect on complex peptides insulin (~5800 Da, 3 disulfides) and hepcidin (~2800 Da, 4 disulfides), as well as on the small protein lysozyme (~14,300 Da, 4 disulfides).

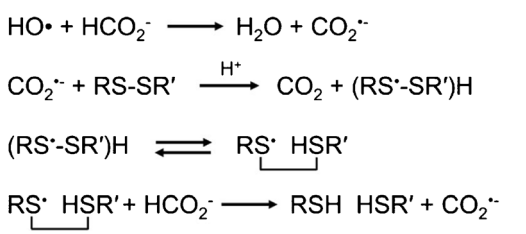

Scheme 1 Proposed reaction scheme for disulfide reduction of formate-containing solutions electrosprayed under corona discharge conditions, simplified from prior radiolysis experiments outlined by Favaudon et al. [25]

To confirm the formate-mediated ISR mechanism, and investigate the effect of acidic pH, insulin and hepcidin were dissolved in solutions **1**–**5** and electrosprayed at 4 kV. Reduction of the two insulin interchain disulfides liberates the individual A- and B-chains, and Fig. 5a depicts the resulting intensity of the insulin B-chain, measured as the 4+ ion. Note that all subsequent experiments were performed at a flow rate of 5 μL min^{-1}. Minimal abundance was observed from solution **1**, which contained no formate and thus served as the ISR negative control. Small increases in B-chain intensity were measured from solutions **3** and **4**, consistent with a

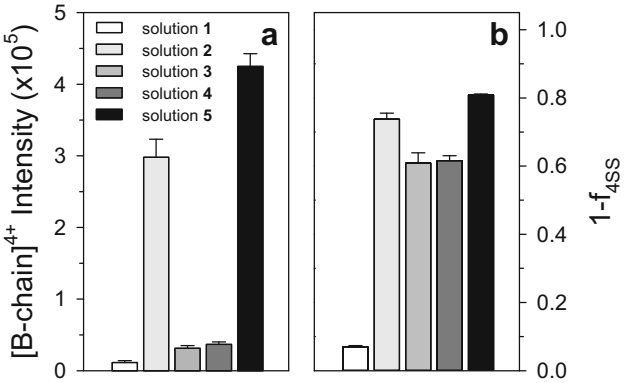

Fig. 5 Solvent effects on ISR of complex peptides. (a) Insulin B-chain intensity from various solution conditions (see "Experimental") when sprayed at 4 kV, integrated over *m/z* 849.5–852.5. (b) Fraction of total hepcidin with at least one disulfide reduced, depicted as one *minus* the fraction containing all 4 disulfides. Solution and instrument conditions are identical to those in panel (a). Error bars represent the standard deviation of triplicate measurements

formate-mediated mechanism of ISR. The accumulation of isolated B-chain is a useful marker of extensive insulin reduction, however is blind to molecules undergoing only one disulfide reduction (or one interchain and the intra-A-chain bond). Ion mobility has been used to detect conformational changes accompanying disulfide reduction by ISR [21]. The arrival time distributions for insulin sprayed from solutions **3** and **4** revealed the appearance of an extended conformer (ESM Fig. S7), presumably the result of partial ISR. Alternatively, when insulin was sprayed from formic acid–containing solutions at pH 2.7 (solutions **2** and **5**), increases in the extended conformer population, as well as the appearance of a more extended conformer, were observed (ESM Fig. S7). In addition, a dramatic increase in B-chain abundance was measured (Fig. 5a). These findings are consistent with those of Favaudon and coworkers [25], who observed that protein disulfide reduction rapidly goes to completion under acidic conditions whereas neutral pH results in only partial reduction. The need for both formate-containing solutions at low pH and corona discharge to achieve complete insulin reduction was supported by measurements on the Fusion Lumos (ESM Fig. S8). A similar trend was seen for hepcidin (Fig. 5b), whereby the presence of formate significantly increased the proportion of the sample which experienced at least one disulfide reduction, with a further increase facilitated at low pH. Figure S9 (see ESM) shows that while hepcidin sprayed from all solutions underwent compaction with increasing ESI voltage, reported to result from ISR [21], the increase in hepcidin reduction at low pH was manifested mostly through an increase in the doubly disulfide bonded state.

Radiolysis studies of protein disulfide bond reduction in formate solutions reveal a pH dependence; reduction of bovine serum albumin is more efficient at pH 4 than at pH 5.5, and the optimal pH for ribonuclease reduction is 2.5 [26]. We observed a similar trend during CD-ESI of lysozyme (Lyz). Figure 6 shows the collision cross section (CCS) of the Lyz 7+ charge state measured under various solution and instrument conditions. The 7+ charge state was chosen for conformational analysis as it is abundant in the native Lyz mass spectrum, and the relatively low charge density minimizes potential structural alterations due to coulombic repulsion in the gas phase [4, 45]. Under non-ISR conditions (no formate, low voltage), a broad distribution was observed with a maximum near 1375 $Å^2$, similar to previous measurements [11, 45, 46]. Comparison of panels b/c and d/e in Fig. 6 revealed increased CCS in the presence of acid, consistent with our peptide experiments. The extended conformer around 1475 $Å^2$ in Fig. 6e was ascribed to a partially reduced protein state as it was also observed in a Lyz sample partially reduced by DTT, and was nearly absent in a fully DTT-reduced sample (Fig. 6). A recent investigation into Lyz structural transitions [46] showed that the solution-phase conformation was not affected by acid

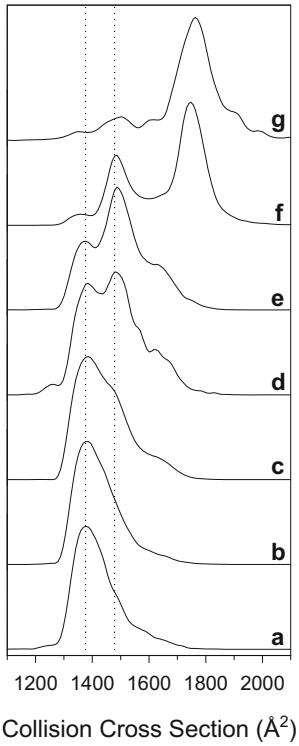

Fig. 6 Collision cross section profiles for the lysozyme 7+ charge state measured under different solution and ESI voltage conditions. (a) solution **1**, 2 kV; (b) solution **4**, 2 kV; (c) solution **5**, 2 kV; (d) solution **4**, 4 kV; (e) solution **5**, 4 kV; (f) 25 mM DTT, 70 °C for 5 min, 2 kV; (g) 25 mM DTT, 70 °C for 30 min, 2 kV. Vertical dotted lines are intended as alignment aids for feature comparison

type; however, extended gas-phase conformers were observed by ion mobility predominantly when formic acid was used. Protein unfolding within the ESI droplet due to charge repulsion was argued to be the cause [46]; however, our results suggest that disulfide reduction was the likely culprit. Overall, the complex peptide and protein results support the formate-mediated ISR mechanism discerned from the oxytocin experiments. They also suggest that the increased reduction observed at low pH may not be due solely to the need for thiyl radical protonation (Scheme 1, step 2), but also to increased disulfide solvent accessibility resulting from higher-order structure disruption.

Corona discharge conditions are generally avoided in ESI-MS experiments due to degradation of analyte signal. Disulfide ISR however does not require extreme capillary voltages; most reports utilize values that are within the normal operating range recommended by the instrument manufacturers [18–21]. Using pure peptide solutions, we observed an approximate 4-fold intensity decrease upon increasing capillary voltage from 2 to 4 kV, likely due to in-source fragmentation, while the background signal and charge state distributions remained largely unaffected (ESM Fig. S10). In many experiments, information gleaned from ISR regarding cysteine linkage patterns would outweigh this small reduction in analyte signal.

Conclusions

Disulfide ISR can be utilized to elucidate complex cysteine linkage patterns in LC-MS experiments without the need for chemical reduction and alkylation; however, mechanistic details have heretofore been scarce. We demonstrated on multiple mass spectrometers, with disparate source geometries, that disulfide reduction within the electrospray source results from corona discharge applied to formate-containing solutions. Variance of instrument parameters known to modulate electric discharge during ESI, such as nebulizer gas type, was shown to dramatically affect the degree of ISR. However, rigorous examination of solution conditions revealed formate as an obligatory additive in order to achieve appreciable disulfide reduction. Electrospraying from acidic solution resulted in enhanced oxytocin ISR only under the most extreme conditions, and only when formic acid was used as the titrant. For more complex polypeptides—insulin, hepcidin, and lysozyme—lowering the pH resulted in increased disulfide reduction when compared to neutral solutions, ostensibly due to acid-induced higher-order structure disruption. Drawing on prior radiolysis work [23–26], our results support the proposal of disulfide reduction by carboxyl radical anion, formed via H abstraction from formate by hydroxyl radical produced within the ESI source during corona discharge. Insight into the mechanism of disulfide in-source reduction is critical for MS practitioners wishing to take advantage of the phenomenon, as well as those wanting to avoid biomolecule modification during analysis.

Acknowledgements The authors would like to thank Dr. Christopher Miles for helpful discussions.

Compliance with ethical standards

Conflict of interest The authors declare that they have no conflicts of interest.

References

1. Fenn JB. Electrospray wings for molecular elephants (Nobel lecture). Angew Chem Int Ed. 2003;42:3871–94. https://doi.org/10.1002/anie.200300605.
2. Heck AJR, van den Heuvel RHH. Investigation of intact protein complexes by mass spectrometry. Mass Spectrom Rev. 2004;23:368–89. https://doi.org/10.1002/mas.10081.
3. Sharon M, Robinson CV. The role of mass spectrometry in structure elucidation of dynamic protein complexes. Annu Rev Biochem. 2007;76:167–93. https://doi.org/10.1146/annurev.biochem.76.061005.090816.
4. Vahidi S, Stocks BB, Konermann L. Partially disordered proteins studied by ion mobility-mass spectrometry: implications for the preservation of solution phase structure in the gas phase. Anal Chem. 2013;85:10471–8.
5. Boys BL, Kuprowski MC, Konermann L. Protein oxidative modifications during electrospray ionization: solution phase electrochemistry or corona discharge-induced radical attack? Anal Chem. 2009;81:4027–34. https://doi.org/10.1021/ac900243p.
6. Kumar M, Chatterjee A, Khedkar AP, Kusumanchi M, Adhikary L. Mass spectrometric distinction of in-source and in-solution pyroglutamate and succinimide in proteins: a case study on rhG-CSF. J Am Soc Mass Spectrom. 2012;24:202–12. https://doi.org/10.1007/s13361-012-0531-7.
7. Loo JA, Udseth HR, Smith RD. Collisional effects on the charge distribution of ions from large molecules, formed by electrospray-ionization mass spectrometry. Rapid Commun Mass Spectrom. 1988;2:207–10. https://doi.org/10.1002/rcm.1290021006.
8. Lloyd JR, Hess S. A corona discharge initiated electrochemical electrospray ionization technique. J Am Soc Mass Spectrom. 2009;20:1988–96. https://doi.org/10.1016/j.jasms.2009.07.021.
9. Ikonomou MG, Blades AT, Kebarle P. Electrospray mass spectrometry of methanol and water solutions suppression of electric discharge with SF_6 gas. J Am Soc Mass Spectrom. 1991;2:497–505. https://doi.org/10.1016/1044-0305.
10. Kebarle P, Verkerk UH. Electrospray: from ions in solution to ions in the gas phase, what we know now. Mass Spectrom Rev. 2009;28:898–917. https://doi.org/10.1002/mas.20247.
11. Maleknia SD, Downard KM. Advances in radical probe mass spectrometry for protein footprinting in chemical biology applications. Chem Soc Rev. 2014;43:3244–58. https://doi.org/10.1039/c3cs60432b.
12. Buxton GV, Greenstock CL, Helman WP, Ross AB. Critical review of rate constants for reactions of hydrated electrons, hydrogen atoms and hydroxyl radicals (·OH/·O−) in aqueous solution. J Phys Chem Ref Data. 1988;17:513–886. https://doi.org/10.1063/1.555805.
13. Betz SF. Disulfide bonds and the stability of globular proteins. Protein Sci. 1993;2:1551–8. https://doi.org/10.1002/pro.5560021002.
14. Gorman JJ, Wallis TP, Pitt JJ. Protein disulfide bond determination by mass spectrometry. Mass Spectrom Rev. 2002;21:183–216. https://doi.org/10.1002/mas.10025.
15. Xia Y, Cooks RG. Plasma induced oxidative cleavage of disulfide bonds in polypeptides during nanoelectrospray ionization. Anal Chem. 2010;82:2856–64. https://doi.org/10.1021/ac9028328.
16. Stinson CA, Xia Y. Radical induced disulfide bond cleavage within peptides via ultraviolet irradiation of an electrospray plume. Analyst. 2013;138:2840–6. https://doi.org/10.1039/c3an00303e.
17. Kraj A, Brouwer H-J, Reinhoud N, Chervet J-P. A novel electrochemical method for efficient reduction of disulfide bonds in peptides and proteins prior to MS detection. Anal Bioanal Chem. 2013;405:9311–20. https://doi.org/10.1007/s00216-013-7374-3.
18. Nicolardi S, Deelder AM, Palmblad M, van der Burgt YE. Structural analysis of an intact monoclonal antibody by online electrochemical reduction of disulfide bonds and Fourier transform ion cyclotron resonance mass spectrometry. Anal Chem. 2014;86:5376–82. https://doi.org/10.1021/ac500383c.
19. Cramer CN, Kelstrup CD, Olsen JV, Haselmann KF, Nielsen PK. Complete mapping of complex disulfide patterns with closely-spaced cysteines by in-source reduction and data-dependent mass spectrometry. Anal Chem. 2017;89:5949–57. https://doi.org/10.1021/acs.analchem.7b00424.
20. Cramer CN, Kelstrup CD, Olsen JV, Haselmann KF, Nielsen PK. Generic workflow for mapping of complex disulfide bonds using in-source reduction and extracted ion chromatograms from data-dependent mass spectrometry. Anal Chem. 2018;90:8202–10. https://doi.org/10.1021/acs.analchem.8b01603.
21. Stocks BB, Melanson JE. In-source reduction of disulfide-bonded peptides monitored by ion mobility mass spectrometry. J Am Soc

Mass Spectrom. 2018;29:742–51. https://doi.org/10.1007/s13361-018-1894-1.
22. Pei J, Hsu CC, Zhang R, Wang Y, Yu K, Huang G. Unexpected reduction of iminoquinone and quinone derivatives in positive electrospray ionization mass spectrometry and possible mechanism exploration. J Am Soc Mass Spectrom. 2017;28:2454–61. https://doi.org/10.1007/s13361-017-1770-4.
23. Elliot AJ, Sopchyshyn FC. The radiolysis of aqueous solutions containing dithiotreitol and oxidized dithiothreitol. Radiat Phys Chem. 1982;19:417–26. https://doi.org/10.1016/0146-5724(82)90131-5.
24. Elliot AJ, Simsons AS, Sopchyshyn FC. Radiolysis of solutions containing organo-disulphides. Radiat Phys Chem. 1984;23:377–84. https://doi.org/10.1016/0146-5724(84)90124-9.
25. Favaudon V, Tourbez H, Houée-Levin C, Lhoste J-M. $CO_2^{\cdot-}$ radical induced cleavage of disulfide bonds in proteins. A γ-ray and pulse radiolysis mechanistic investigation. Biochemistry. 1990;29:10978–89. https://doi.org/10.1021/bi00501a016.
26. Koch CJ, Raleigh JA. Radiolytic reduction of protein and nonprotein disulfides in the presence of formate: a chain reaction. Arch Biochem Biophys. 1991;287:75–84. https://doi.org/10.1016/0003-9861(91)90390-5.
27. Sun Y, Vahidi S, Sowole MA, Konermann L. Protein structural studies by traveling wave ion mobility spectrometry: a critical look at electrospray sources and calibration issues. J Am Soc Mass Spectrom. 2015;27. https://doi.org/10.1007/s13361-015-1244-5.
28. Chalkley RJ, Baker PR, Medzihradszky KF, Lynn AJ, Burlingame AL. In-depth analysis of tandem mass spectrometry data from disparate instrument types. Mol Cell Proteomics. 2008;7:2386–98. https://doi.org/10.1074/mcp.M800021-MCP200.
29. Li G, Yin Y, Huang G. Increased disulfide peptide sequence coverage via "cleavage on/off" switch during nanoelectrospray. RSC Adv. 2014;4:59650–4. https://doi.org/10.1039/c4ra12386g.
30. Abonnenc M, Qiao L, Liu B, Girault HH. Electrochemical aspects of electrospray and laser desorption/ionization for mass spectrometry. Annu Rev Anal Chem. 2010;3:231–54. https://doi.org/10.1146/annurev.anchem.111808.073740.
31. Zinck N, Stark AK, Wilson DJ, Sharon M. An improved rapid mixing device for time-resolved electrospray mass spectrometry measurements. ChemistryOpen. 2014;3:109–14. https://doi.org/10.1002/open.201402002.
32. Kanev IL, Mikheev AY, Shlyapnikov YM, Shlyapnikova EA, Morozova TY, Morozov VN. Are reactive oxygen species generated in electrospray at low currents? Anal Chem. 2014;86:1511–7. https://doi.org/10.1021/ac403129f.
33. Smith RD, Loo JA, Ogorzalek Loo RR, Busman M, Udseth HR. Principles and practice of electrospray ionization-mass spectrometry for large polypeptides and proteins. Mass Spectrom Rev. 1991;10. https://doi.org/10.1002/mas.1280100504.
34. Van Berkel GJ, Kertesz V. Using the electrochemistry of the electrospray ion source. Anal Chem. 2007;79:5510–20. https://doi.org/10.1021/ac071944a.
35. Liu Y-H, Konermann L. Conformational dynamics of free and catalytically active thermolysin are indistinguishable by hydrogen/deuterium exchange mass spectrometry. Biochemistry. 2008;47:6342–51. https://doi.org/10.1021/bi800463q.
36. Nshanian M, Lakshmanan R, Chen H, Ogorzalek Loo RR, Loo JA. Enhancing sensitivity of liquid chromatography-mass spectrometry of peptides and proteins using supercharging agents. Int J Mass Spectrom. 2018;427:157–64. https://doi.org/10.1016/j.ijms.2017.12.006.
37. Eshraghi J, Chowdhury SK. Factors affecting electrospray ionization of effluents containing trifluoroacetic acid for high-performance liquid chromatography/mass spectrometry. Anal Chem. 1993;65:3528–33. https://doi.org/10.1021/ac00071a035.
38. Li G, Pei J, Yin Y, Huang G. Direct sequencing of a disulfide-linked peptide with electrospray ionization tandem mass spectrometry. Analyst. 2015;140:2623–7. https://doi.org/10.1039/c5an00011d.
39. Wang W, Wang S, Liu F, Zheng W, Wang D. Optical study of OH radical in a wire-plate pulsed corona discharge. Spectrochim Acta, Part A. 2006;63:477–82. https://doi.org/10.1016/j.saa.2005.05.033.
40. Xu G, Chance MR. Hydroxyl radical-mediated modification of proteins as probes for structural proteomics. Chem Rev. 2007;107:3514–43. https://doi.org/10.1021/cr0682047.
41. Tong X, Wren JC, Konermann L. γ-ray-mediated oxidative labeling for detecting protein conformational changes by electrospray mass spectrometry. Anal Chem. 2008;80:2222–31. https://doi.org/10.1021/ac702321r.
42. Adams GE, Redpath JL, Bisby RH, Cundall RB. The use of free radical probes in the study of mechanisms of enzyme inactivation. Isr J Chem. 1972;10:1079–93. https://doi.org/10.1002/ijch.197200116.
43. Wu Z, Ahmad R, Armstrong DA. Formation of lipoamide anion radicals by hydroxyl, formate, and alcohol radicals at ph 6-9. Radiat Phys Chem. 1984;23:251–7. https://doi.org/10.1016/0146-5724(84)90116-X.
44. Raleigh JA, Koch CJ. Importance of thiols in the reductive binding of 2-nitroimidazoles to macromolecules. Biochem Pharmacol. 1990;40:2457–64. https://doi.org/10.1016/0006-2952(90)90086-Z.
45. Valentine SJ, Anderson JG, Ellington AD, Clemmer DE. Disulfide-intact and -reduced lysozyme in the gas phase: conformations and pathways of folding and unfolding. J Phys Chem B. 1997;101:3891–900. https://doi.org/10.1021/jp970217o.
46. Lee JW, Kim HI. Investigating acid-induced structural transitions of lysozyme in an electrospray ionization source. Analyst. 2015;140:661–9. https://doi.org/10.1039/c4an01794c.